

On the heat capacities of Ta₂AlC, Ti₂SC, and Cr₂GeC

Monika K. Drulis,¹ H. Drulis,^{1,a)} A. E. Hackemer,¹ O. Leaffer,² J. Spanier,² S. Amini,²
M. W. Barsoum,² T. Guilbert,³ and T. El-Raghy⁴

¹Polish Academy of Sciences, Trzebiatowski Institute of Low Temperature and Structure Research, P.O. Box 1410, 50-950 Wrocław 2, Poland

²Department of Materials Science and Engineering, Drexel University, Philadelphia, Pennsylvania 19104, USA

³Saclay Center, CEA, F-91191 Gif-Sur-Yvette, France

⁴3-ONE-2, Voorhees, New Jersey 08043, USA

(Received 8 February 2008; accepted 10 May 2008; published online 24 July 2008)

Herein we report on the heat capacities c_p of bulk predominantly single-phase polycrystalline samples of Ti₂SC and Cr₂GeC in the 3–1500 K temperature range and Ta₂AlC in the 3–260 K range. At temperatures up to 10 K the main contributors to c_p for Ta₂AlC and Cr₂GeC are electronic, with electronic coefficients γ of 7.13 and 26.12 mJ/mol K², respectively. The latter is exceptionally high and is a record for this family of layered ternary carbides and nitrides also known as the MAX phases. In Ti₂SC another low-temperature contribution—in addition to a γ of 3.8 mJ/mol K²—is manifested by an upturn in c_p/T observed at the lowest temperatures. This feature, appearing as a Schottky-like anomaly, has a local maximum near 4.5 K and an intensity of $\sim 1.9 \times 10^{-2}$ J/mol K. A defect concentration of $\sim 3 \times 10^{21}$ /mol presumably on the S-sublattice, is proposed as the origin of a two-level energy system responsible for this anomaly. As in previous work on these compounds, the lattice contributions to c_p in all compounds are analyzed using the Debye and Einstein model approximations. The main effect of increasing the atomic number of the transition metal is a reduction in Debye temperature. © 2008 American Institute of Physics. [DOI: 10.1063/1.2956511]

I. INTRODUCTION

The ternary carbides $M_{n+1}AX_n$ (where M is an early transition metal, A is an A group element, and X=C or N) (MAX) comprise a family of layered hexagonal (space group $P6_3/mmc$) compounds.^{1,2} By now it is fairly well established that these phases possess an unusual, and sometimes unique, set of properties.^{2–13} In general they have relatively low thermal expansion coefficients, and good thermal and electrical conductivities.^{3,9,13} They are relatively soft, readily machinable, thermal shock resistant, and damage tolerant. At higher temperatures, they undergo a brittle-to-plastic transition.^{3–6,11} Some such as Ti₂AlC are exceptionally oxidation resistant and are candidate materials for high-temperature structural industrial applications.¹⁴

Generally, accurate knowledge of the constant-pressure heat capacity c_p of a material, over its entire stability regime, is of vital scientific and technical importance. Without it a compound's thermodynamic parameters cannot be calculated. Furthermore, low-temperature c_p measurement is an established technique to experimentally determine the density of states (DOS) at the Fermi level. The latter in turn is crucial for comparison with DOS calculated from first-principles methods. By using such density-functional theoretical simulation methods, accurate theoretical predictions of values of bulk moduli and the DOS can be made.^{15–19}

By now it is well established that the low-temperature c_p of the MAX phases can be described by the well-known relationship^{20–25}

$$c_p \approx c_v = \gamma T + \beta T^3, \quad (1)$$

where γ and β are the coefficients of electronic and lattice contributions to the heat capacity, respectively, and c_v is the heat capacity at constant volume and is assumed throughout this paper to be equal to c_p .

The coefficient β is related to the Debye temperature Θ_D by

$$\theta_D^3 = \frac{12\pi^4 R}{15\beta} N_D, \quad (2)$$

where $N_D = 3r$ is the number of Debye-like modes, r is the number of atoms per f.u., and R is the molar gas constant.

Strictly speaking, Eq. (2) is only valid for a pure element or r atoms of equal mass. We have argued in several papers^{22–25} that $N_D = 3r$ is an oversimplification for the MAX phases. For example, we have also shown that N_D for the M_2AX phases is < 12 . A similar situation is encountered in metal hydrides containing a variable number of light interstitial atoms without a concomitant change in the measured β ; including them in N_D , a false variation of Θ_D would be obtained.²⁶ Moreover, while c_p for some of the MAX phases have already been measured,^{22–25,27} that for the vast majority of the more than 50+ compounds have not. A preliminary, short report on the c_p of Ti₂SC in the 3–300 K temperature range will be reported elsewhere.²⁸ In that work we showed that if one assumes a simple Debye model, viz., $N_D = 3r$, Θ_D is 765 K. Herein we present a more comprehensive measurement of c_p , collected over a wider temperature range, along with a more nuanced interpretation of c_p .

^{a)}Electronic mail: drulis@int.pan.wroc.pl.

The purpose of this paper is thus to report on, and interpret, the temperature variations of c_p and Ti_2SC and Cr_2GeC in the 3–1500 K temperature range and Ta_2AlC in the narrower range of 3–260 K.

II. EXPERIMENTAL AND MODELING DETAILS

The sample fabrication details for Ti_2SC , Ta_2AlC , and Cr_2GeC can be found elsewhere.^{29–31} In brief, the Ta_2AlC samples were fabricated by hot isostatically pressing at 1100 °C for 0.3 h under ~ 70 MPa from Ta_2AlC powders ($>92\%$, 3-ONE-2, Voorhees, NJ). X-ray diffraction phase-pure, -325 mesh Ti_2SC powders (3-ONE-2, Voorhees, NJ) were hot pressed in a graphite-heated, vacuum atmosphere hot press (HP) (series 3600, Centorr Vacuum Industries, Somerville, MA). The powder was poured and wrapped in graphite foil, which, in turn, was placed in a graphite die and heated at 10 °C/min to 1500 °C for 5 h.²⁹

Phase-pure -325 mesh Ti_2SC powders (3-ONE-2, Voorhees, NJ) were hot pressed in a graphite-heated, vacuum atmosphere HP. The powders were held for ~ 5 h at 1500 °C under a load that corresponded to a stress of ~ 45 MPa, which was applied at 500 °C and maintained throughout the entire process.³⁰

Stoichiometric powder mixtures of chromium (99% pure, -325 mesh, Alfa Aesar, Ward Hill, MA), germanium (99% pure, -325 mesh, Cerac, Milwaukee, WI), and carbon (99.0% pure, -300 mesh, Alfa Aesar, Ward Hill, MA) were ball milled for 24 h and dried in a low vacuum atmosphere for 24 h at 180 °C. The mixed powders were poured and wrapped in graphite foil, placed in a graphite die and heated in the HP at 10 °C/min to 1350 °C and held at temperature for ~ 6 h. A load, corresponding to a stress of ~ 45 MPa, was applied at 500 °C and maintained throughout the heating process.³¹

The low-temperature c_p measurements—the details of which can be found in Ref. 23 were carried out between 3 and 260 K, using two different adiabatic calorimeters. The c_p for each sample was obtained by subtracting the addenda contributions. The high-temperature c_p measurements were performed with a Setaram-Multi HTC high-temperature and high-sensitivity calorimeter. Compared to more conventional Differential Scanning Calorimetry (DSC) devices, this apparatus enables us to work under inert gas up to 1420 °C, with typical heating/cooling rates ranging from 1 up to 10 K/min. The samples used were cylindrical shaped specimens 5 mm diameter and 12 mm height (typical sample weight ~ 1 g). This facility makes it possible to measure the heat flow between the tested sample and an inert reference sample. Temperature and enthalpy measurements were calibrated using known melting points of several standard metals (In, Al, Au, etc.). The tests were carried out under purified He atmospheres, with a flow rate of ~ 0.6 l/h. For these conditions, the accuracy of the measurement is estimated to be around $\pm 5\%$. The c_p measurements of the samples tested were derived by applying the “continuous method.”³² For all the measurements, the samples were first heated at 473 K for 1 h, followed by a heating at 3 K/min up to 1473 K at which time the furnace is cooled down to 293 K.

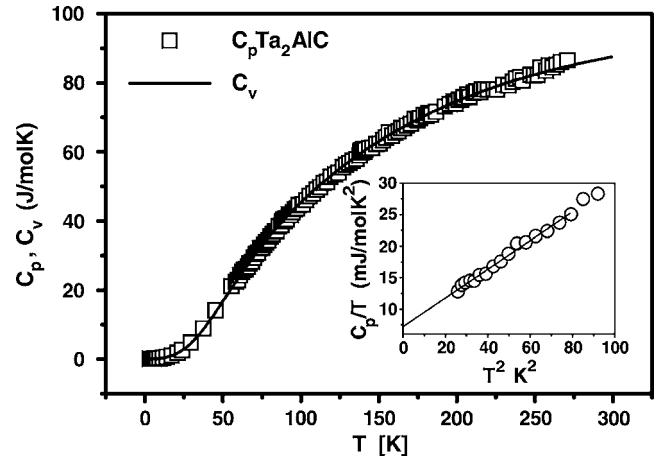


FIG. 1. Temperature dependencies of experimental c_p (open squares) and calculated c_p (solid line) results for Ta_2AlC sample in the 3–260 K temperature range. Inset details c_p/T vs T^2 plots in the 3–10 K temperature range.

Density-functional theoretical simulations of electronic structure and lattice dynamics were performed using the Vienna *ab initio* simulation package³³ (VASP) as implemented within MEDEA.³⁴ The Kohn–Sham equations were solved using the projector augmented wave^{35,36} and the generalized gradient approximation.³⁷ The energy minimized unit cells were calculated using a selected convergence criteria for the electronic iterations (10^{-6}) and for ionic relaxations (0.005 eV/Å). Hellman–Feynman forces and the dynamical matrix were computed using MEDEA’s PHONON module, which uses the so-called direct method.³⁸ The heat capacity at constant volume was calculated directly from the phonon DOS. Convergence of the phonon modes was checked with respect to k -mesh and to supercell size.

III. RESULTS AND DISCUSSION

A. Ta_2AlC

The temperature dependence of c_p for Ta_2AlC is presented in Fig. 1. Shown in the inset is a plot of c_p/T vs T^2 , from which it is obvious that a straight line results, confirming that Eq. (1) describes c_p for this compound. The values of γ and β calculated from the inset in Fig. 1 are listed in Table I, together with the DOS at the Fermi level calculated from γ . Also included are recently published results for V_2AlC , Ti_2AlC , Cr_2AlC ,²⁴ and Nb_2AlC (Ref. 27) for comparison.

Since the transition metals V, Nb, and Ta are in the same column in the Periodic Table, it is not too surprising that at 6, 7.5, and 5.06 (eV unit cell)⁻¹, the DOSs at the Fermi level of Ta_2AlC , V_2AlC , and Nb_2AlC , respectively, are not too different. In contradistinction, given the large differences in atomic mass, it is again not surprising that the lattice dynamics are quite different. The Debye temperatures of the three compounds drop—from 625 K for V_2AlC to 540 K for Nb_2AlC to 281 K for Ta_2AlC —as their atomic mass increases.

As described in detail in our previous works,^{22–25} for most MAX compounds, N_D is not equal to $3r$, viz., 12. We believe that the same is true here for Ta_2AlC . Because of the

TABLE I. Summary of the electronic and lattice coefficients measured herein for Ta₂AlC, Ti₂SC, and Cr₂GeC. Also included, for comparison's sake, are previous results for V₂AlC, Ti₂AlC, Cr₂AlC, and Nb₂AlC (Ref. 27).

Compound	γ (mJ/mol K ²)	$N(E_F)$ (eV UC) ⁻¹	β (J/mol K ⁴)	N_D	Θ_D (K)	N_E (K)	Θ_E (K)
Ta ₂ AlC	7.13	6.0	22.5×10^{-5}	6	281	2	304
V ₂ AlC ^a	8.83	7.5	2.46×10^{-5}	9	625	4	665
Nb ₂ AlC ^b	6.0	5.06	4.90×10^{-5}	12	540	1	1000
Cr ₂ GeC	26.12	22.0	7.46×10^{-5}	9	429	2	168
Cr ₂ AlC ^a	17.15	14.6	2.85×10^{-5}	9	594	1	260
						1	1000
Ti ₂ SC	3.8	3.2	...	11	631	1	278
Ti ₂ AlC ^a	4.6	3.9	1.87×10^{-5}	9	672	3	270

^aReference 24.

^bReference 27.

large mass differential between Ta, on the one hand, and Al and C, on the other, it is likely that the modes possessing acousticlike dispersions mainly involve displacements of Ta atoms, and these modes, viz., $N_D=6$, are largely responsible for the lattice contribution to c_p at the lowest temperatures. Like other MAX phases,²⁴ the contributions of the other atoms to c_p can be represented by Einstein-like modes. Said otherwise, c_p can be approximated by the sum of three components,

$$c_v = \gamma T + N_D c_{V(D)} + N_E c_{V(E)}, \quad (3)$$

where the first two terms on the right-hand side are defined in Eq. (1). The third term reflects the contribution to c_v from Einstein-like vibration modes,

$$N_E c_{v(E)} = \frac{N_E R}{4(\Theta_E/T)^2} \text{csch}^2\left(\frac{1}{2\Theta_E/T}\right), \quad (4)$$

where Θ_E is the Einstein temperature.

Assuming $\gamma=7.13$ mJ/mol K², $N_D=6$ in Eq. (3), and selecting different values of N_E , the best fit of the experimental c_p data in the wide 15–270 K temperature range is obtained by selecting two low-energy Einstein-like modes ($N_E^L=2$) and four high-energy Einstein modes ($N_E^H=4$). Least squares fits of the data with Θ_D and low- and high-energy Einstein mode temperatures Θ_E^L and Θ_E^H yields $\Theta_D=281$ K, $\Theta_E^L=304$ K, and $\Theta_E^H=665$ K. The agreement between experimental (open squares in Fig. 1) and calculated data (full line in Fig. 1) for the most part is quite good.

In contradistinction, for V₂AlC,²⁴ the lattice contribution to c_p is well described by nine Debye-like and three Einstein-like modes over the entire temperature range. This indirectly confirms the observation that the distribution of lattice vibrational energy between Debye-like and Einstein-like modes depends on the atomic mass ratios in a given compound and confirms that the dispersion characteristics of the low-energy optical phonon branches are acousticlike, as seen in the calculated phonon dispersions for Ta₂AlC, Cr₂GeC, and Ti₂SC (shown in Fig. 5).

B. Cr₂GeC

The c_p measurements for Cr₂GeC are shown in Fig. 2. A plot of c_p/T vs T^2 (upper inset in Fig. 2) yields $\gamma=26.12$ mJ/mol K² and $\beta=7.46 \times 10^{-5}$ J/mol K⁴. Analysis of the c_p results for Cr₂GeC was carried out in a manner similar to that for Ta₂AlC. However, because atomic masses Cr and Ge are close to each other, it is reasonable to assume that their lattice vibrational energies have the same Debye-like characteristics and number of N_D modes to be 9. Before carrying out the full-fitting procedure, the rough number of Einstein modes and their energies at low temperatures need to be estimated. To do so, we plot $[(c_p - \gamma T)/T^3 - \beta]$ vs T (lower inset in Fig. 2). This curve is well described if one assumes $N_E=1$, with a $\Theta_E=168$ K.

Taking $\gamma=26.12$ mJ/mol K², the fit of c_p with Eq. (3) in the temperature range measured was attempted. The least squares procedure yields a $\Theta_D=429$ K and $\Theta_E=168$ K for $N_D=9$ and $N_E=1$, respectively. Unfortunately, good agreement between experimental and calculated curves was obtained only in the 4–170 K temperature range. Further ef-

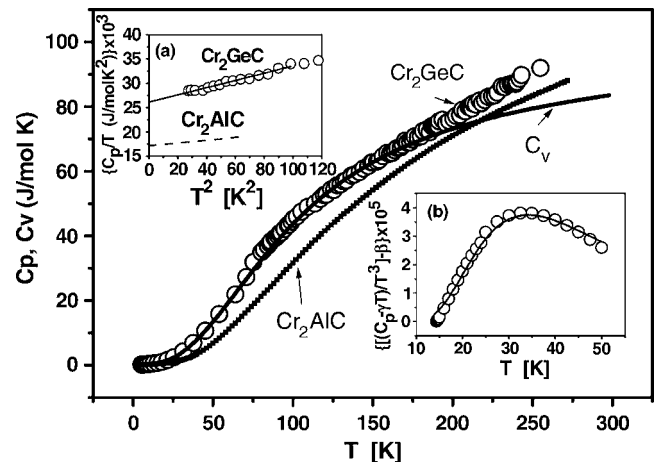


FIG. 2. Temperature dependencies of experimental c_p (open circles) and calculated c_v (solid line) results for Cr₂GeC sample in the 3–260 K temperature range. Top inset plots c_p/T vs T^2 in the 3–20 K temperature range. Lower inset plots $[(c_p - \gamma T)/T^3 - \beta]$ vs T . Also plotted for the sake of comparison are the results for Cr₂AlC from Ref. 24.

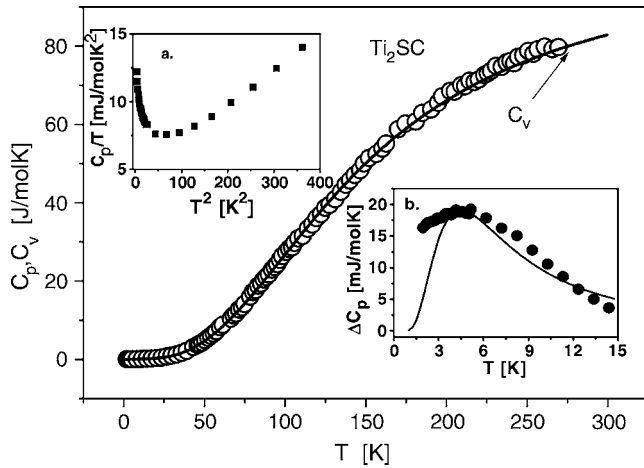


FIG. 3. Temperature dependencies of experimental c_p (open circles) and calculated c_v (solid line) results for Ti_2SC sample in the 3–260 K temperature range. Top inset plots c_p/T vs T^2 in the 3–10 K temperature range. Lower inset plots $\Delta c_p T = (c_p^{\text{exp}} - c_v^{\text{cal}})$.

forts to fit c_p at temperatures $T > 170$ K were unsuccessful, in spite of fact that there are two additional modes—presumably connected with the C atoms—that are not accounted for. The reason for the large increase of c_p in the 170–260 K temperature range is not understood. The same problem was encountered for Cr_2AlC :²⁹ the agreement between the experimental and calculated values was acceptable only up to about 180 K.

At 22 (eV UC)⁻¹ the DOS at the Fermi level in Cr_2GeC is by far the highest measured to date for a *MAX* phase. Interestingly, with a DOS of 14.6 (eV UC)⁻¹, that of Cr_2AlC is the second highest. It thus appears that the Cr-containing 211 *MAX* phases have quite large DOS at the Fermi level.

C. Ti_2SC

Figure 3 plots c_p vs T in the 3–300 K temperature range; the upper inset plots c_p/T vs T^2 for $T < 20$ K. The visible upturn of c_p/T at the lowest temperatures precludes the direct use of Eq. (1), as done to date for all other *MAX* phases.^{22–25} This upturn indicates that in addition to the electronic γ term, additional low-energy thermal excitations exist. To extract the latter, Eq. (3) was used but *only* in the 10–40 K results. Least squares fitting resulted in a $\gamma \approx 3.8$ mJ/K² mol and a Θ_D equal to 631 K, assuming $N_D = 11$ and $\Theta_E = 278$ K ($N_E = 1$). These parameters describe c_p from 14 up to 260 K (see full line in Fig. 3 and Table I).

Using the same results, the low temperature c_p excess, viz., $\Delta c_p(T) = c_p^{\text{exp}} - c_v^{\text{cal}}$, was plotted versus T in the 3–17 K temperature range (lower inset of Fig. 3). The result is a Schottky-like peak, with a T_{MAX} of 4.5 K and $\Delta c_{\text{MAX}} = 1.9 \times 10^{-2}$ J/mol K. The question arises: What kind of phenomenon is responsible for this contribution?

According to their respective temperature range of importance, the following typical contributions can be considered: (i) nuclear, which is usually recognized by a T^{-2} dependence for T 's < 0.5 K; (ii) spin fluctuation, or paramagnons, characterized by a $T^3 \ln T$ term; (iii) magnons, which are related to some magnetic transition or anomalies; (iv) heavy fermion quasiparticles, Kondo effect, spin glass,

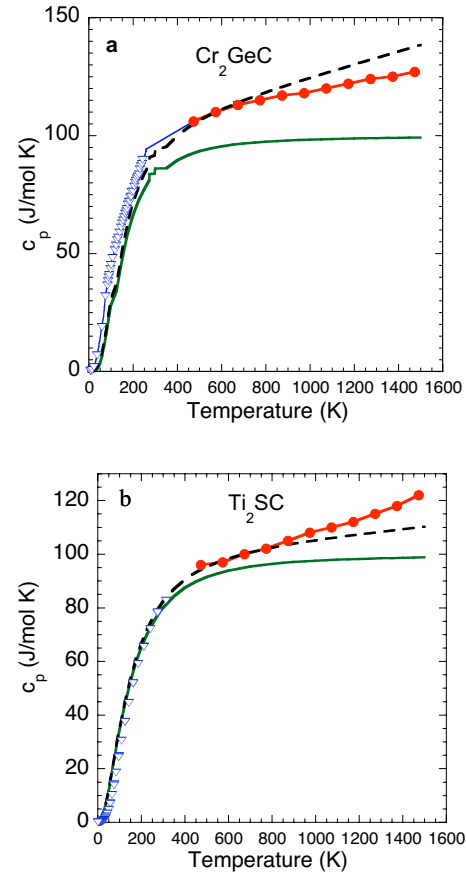


FIG. 4. (Color online) Temperature dependencies of c_p at low temperatures (open triangles), high temperatures (solid circles), lattice *ab initio* (solid line), and the latter plus γT (dashed line), where γ is experimentally obtained and listed in Table I for (a) Cr_2GeC and (b) Ti_2SC .

and finally atomic disorder, like that in a glass matrix. Most of these contributions are either negligible or can be safely ignored because some of them would be detectable only well below the low-temperature limit of our measurements or have different statistics of the thermal populations of the excited state than observed here.

We suggest that the anomalous variation of c_p displayed in insets (a) and (b) of Fig. 3 is due to the disorder in the Ti_2SC atomic structure resembling the disorder in glasses. The existence of glasslike properties in nonglassy materials has been found in many crystalline materials that have been strongly irradiated with high-energy neutrons or in fast ionic conducting solids for example.³⁹ The principal, anomalous low-temperature properties of glasses can be understood in the framework of the two-level system (TLS), which has become the conventional approach in this area.⁴⁰ According to this model, an atom or group of atoms moves in a double-well potential by tunneling (at the lowest temperatures) or by activation processes at relatively higher temperatures.

To describe the TLS contribution to c_p , we must assume that activation processes dominate over tunneling in the 3–14 K temperature region. In this case the atom excitations within the TLS interlevels are described by Boltzmann statistics, while their contributions to c_p are described by a Schottky-like function described by

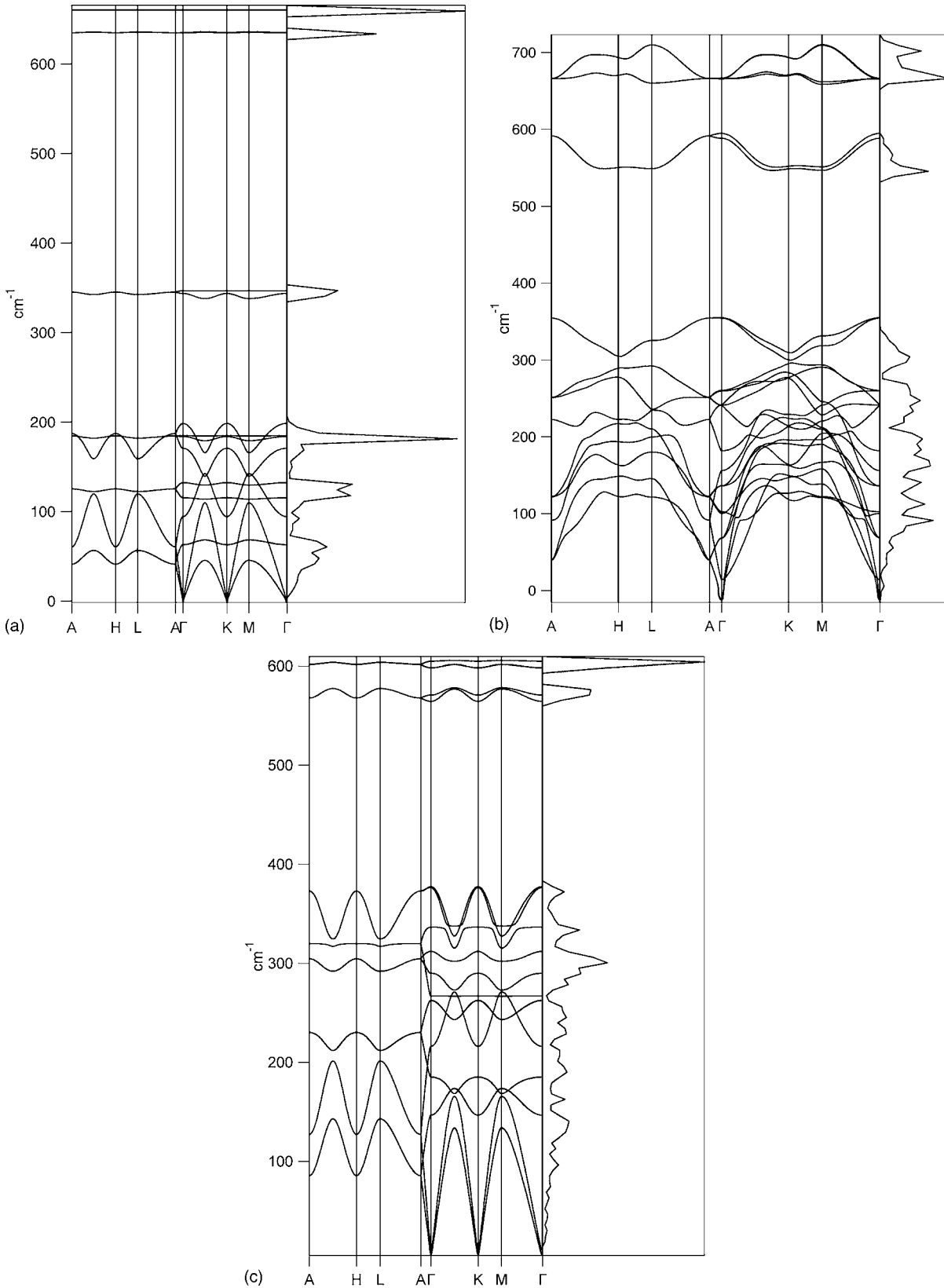


FIG. 5. Calculated phonon dispersions (left) and corresponding vibrational DOS (right) for MAX based on methods described in the text of (a) Ta₂AlC, (b) Cr₂GeC, and (c) Ti₂SC.

$$c_{\text{Sch}} = R(g_i/g_o)(\Delta/T)^2 e^{(\Delta/T)} / [1 + g_i/g_o e^{(\Delta/T)}]^2, \quad (5)$$

where Δ is the energy separation measured in Kelvins, and g_i and g_o are the degeneracies of the energy levels. When g_i

$= g_o$, and for $k_B T \ll \Delta$, then $c_{\text{Sch}} = R(\Delta/T)^2 e^{(\Delta/T)}$, whereas at higher temperatures a typical T^{-2} tail appears.⁴¹ The full line in the lower inset of Fig. 3 describes a Schottky contribution for $g_1/g_o=1$, with an average Δ of 11 K, assuming a con-

centration of TLS defects of $\approx 3 \times 10^{21}$ /mole. While better agreement between experimental and calculated curves could be obtained if a reasonable distribution of Δ values is assumed, such agreement would add little to the discussion. Note that the agreement shown in Fig. 3 does not prove the existence of a TLS but is consistent with it.

Several structural models have appeared recently, which attempt to describe the origin of TLS. Here we adopt the Philips model for $\text{Ge}_{1-x}\text{S}_x$,⁴² who assumed that the TLS phenomenon can be realized in layered solids. Fluctuations of interlayer distances caused by structural defects—in our case most likely on the *S*-sublattice—lead to the deformation of interlayer bonds such that some of them behave as two well potentials. Such lattice defects are also evidenced by an increase in resistivity at the lowest temperatures.²⁸

D. High-temperature and *ab initio* results

Figures 4(a) and 4(b) plot the temperature dependencies of c_p for Cr_2GeC and Ti_2SC , respectively, over the 3–300 K (open triangles) and the 300–1600 K range (solid circles) temperature regimes. The *solid lines* in the figure are the lattice contributions to the heat capacity calculated from density-functional theoretical simulations, some of the results of which are shown in Fig. 5. Note the acousticlike modes in all three compounds in Fig. 5. The *dashed lines* present the calculated lattice contribution plus γT term, where γ is the experimental value reported in Table I. From these results it is clear that when viewed over the entire temperature range, the agreement between theory plus γT and experiment is quite good.

The agreement in the case of Ti_2SC is almost excellent over the 4–1000 K range [Fig. 4(b)]. At higher temperatures the experimental c_p values are higher than theory for reasons that are not entirely clear but may be due to one or more of the following: (i) at higher temperatures, the $c_v \approx c_p$ approximation is no longer a good one, (ii) anharmonic effects that are not accounted for in the density-functional theory (DFT) calculations, and (iii) to the incipient dissociation of the Ti_2SC at higher temperatures.⁴³

IV. SUMMARY AND CONCLUSIONS

Herein we report on and analyze c_p of Ti_2SC and Cr_2GeC in the 3–1500 K temperature range and Ta_2AlC in the 3–260 K range. By also comparing the results with other *MAX* phases we reach the following conclusions.

- (i) The substitution of Ta for V or Nb atoms in $M_2\text{AlC}$ -type compounds has little effect on the electronic properties. The DOS at the Fermi level of Ta_2AlC is 6.0 (eV UC)⁻¹, 7.5 for V_2AlC , and 5.06 (eV UC)⁻¹ for Nb_2AlC , respectively. The high atomic number (atomic mass) of Ta, however, alters the lattice dynamics and results in significantly lower Debye temperatures.
- (ii) For reasons that are unclear, the increase of c_p in Cr_2GeC at $T > 170$ K is so large that we were not able to adequately describe it by the Debye, Einstein, and/or a combination of the two models. A similar

problem was encountered for Cr_2AlC ,²⁴ where the agreement between the experimental and calculated c_p values was good only up to about 180 K. At 26.12 mJ/mol K², γ for Cr_2GeC is by far the highest for any *MAX* phase measured to date. This value, which corresponds to a DOS at the Fermi level of 22 (eV unit cell)⁻¹, is $\approx 50\%$ higher than the previous record of 14.6 (eV UC)⁻¹ reported for another Cr-containing *MAX* phase, viz., Cr_2AlC .

- (iii) In Ti_2SC , a clear visible upturn in c_p/T at the lowest temperatures clearly indicates that, in addition to an ordinary electronic term, additional low-energy thermal excitations must exist. We suggest that these excitations are due to disorder in the Ti_2SC atomic structure reminiscent of a TLS disorder in glasses. To include the TLS contributions to c_p we assumed that in the 3–14 K temperature region, thermally activated processes dominate over tunneling ones, in which case the atom excitations within the TLS interlevels are described by Boltzmann statistics, while their contributions to c_p are described by a Schottky-like function.
- (iv) The agreement between the DFT-calculated and experimental results for Ti_2SC is quite good over the 4–1000 K temperature range. The agreement for Cr_2GeC particularly, at lower temperatures, is less good and is partially related to the larger than expected c_p for Cr_2GeC alluded to above.

ACKNOWLEDGMENTS

The authors are thankful to the Polish State Committee of Scientific Research for financial support under Grant No. 4 T08A 053 24. This work was also partially funded by the Division of Materials Research of the National Science Foundation (Contract No. DMR 0503711).

¹H. Nowotny, *Progress in Solid State Chemistry*, edited by H. Reiss (Pergamon, Oxford, New York, 1970), p. 27.

²M. W. Barsoum and T. El-Raghy, *J. Am. Ceram. Soc.* **79**, 1953 (1996).

³M. W. Barsoum, *Prog. Solid State Chem.* **28**, 201 (2000).

⁴M. W. Barsoum, D. Brodtkin, and T. El-Raghy, *Scr. Mater.* **36**, 535 (1997).

⁵M. W. Barsoum and M. Radovic, in *Encyclopedia of Materials Science and Technology*, edited by K. H. J. Buschow, M. C. Flemings, E. J. Kramer, S. Mahajan, and P. Veyssiere (Elsevier, Amsterdam, 2004).

⁶M. W. Barsoum, M. Ali, and T. El-Raghy, *Metall. Mater. Trans. A* **31**, 1857 (2000).

⁷S. Gupta and M. W. Barsoum, *J. Electrochem. Soc.* **151**, D24 (2004).

⁸M. W. Barsoum and T. El-Raghy, *Am. Sci.* **89**, 336 (2000).

⁹P. Pampuch, J. Lis, L. Stobierski, and M. Tymkiewicz, *J. Eur. Ceram. Soc.* **5**, 283 (1989).

¹⁰P. Pampuch, J. Lis, J. Piekarczyk, and L. Stobierski, *J. Mater. Synth. Process.* **1**, 93 (1993).

¹¹M. W. Barsoum, T. Zhen, S. R. Kalidindi, M. Radovic, and A. Murugiah, *Nat. Mater.* **2**, 107 (2003).

¹²H. I. Yoo, M. W. Barsoum, and T. El-Raghy, *Nature (London)* **407**, 581 (2000).

¹³J. D. Hettinger, S. E. Lofland, P. Finkel, J. Palma, K. Harrell, S. Gupta, A. Ganguly, T. El-Raghy, and M. W. Barsoum, *Phys. Rev. B* **72**, 115120 (2005).

¹⁴M. Sundberg, G. Malmqvist, A. Magnusson, and T. El-Raghy, *Ceram. Int.* **30**, 1899 (2004).

¹⁵Z. Sun, R. Ahuja, S. Li, and J. M. Schneider, *Appl. Phys. Lett.* **83**, 899 (2003).

- ¹⁶J. Wang and Y. Zhou, *Phys. Rev. B* **69**, 214111 (2004).
- ¹⁷J. M. Schneider, Z. Sun, R. Mertens, F. Uestel, and R. Ahuja, *Solid State Commun.* **130**, 445 (2004).
- ¹⁸J. Wang, Y. Zhou, Z. Lin, F. Meng, and F. Li, *Appl. Phys. Lett.* **86**, 101902 (2005).
- ¹⁹G. Hug, M. Jaoun, and M. W. Barsoum, *Phys. Rev. B* **71**, 024105 (2005).
- ²⁰J. C. Ho, H. H. Hamdeh, M. W. Barsoum, and T. El-Raghy, *J. Appl. Phys.* **85**, 7970 (1999).
- ²¹J. C. Ho, H. H. Hamdeh, M. W. Barsoum, and T. El-Raghy, *J. Appl. Phys.* **86**, 3609 (1999).
- ²²M. K. Drulis, A. Czopnik, H. Drulis, and M. W. Barsoum, *J. Appl. Phys.* **95**, 128 (2004).
- ²³M. K. Drulis, A. Czopnik, H. Drulis, J. E. Spanier, A. Ganguly, and M. W. Barsoum, *Mater. Sci. Eng., B* **119**, 159 (2005).
- ²⁴M. K. Drulis, H. Drulis, S. Gupta, M. W. Barsoum, and T. El-Raghy, *J. Appl. Phys.* **99**, 093502 (2006).
- ²⁵M. K. Drulis, H. Drulis, E. Hackemer, A. Ganguly, T. El-Raghy, and M. W. Barsoum, *J. Alloys Compd.* **433**, 59 (2007).
- ²⁶E. F. Westrum, J. B. Hatcher, and D. W. Osborne, *J. Chem. Phys.* **21**, 419 (1953).
- ²⁷S. E. Lofland, J. D. Hettinger, K. Harrell, P. Finkel, S. Gupta, M. W. Barsoum, and G. Hug, *Appl. Phys. Lett.* **84**, 508 (2004).
- ²⁸T. H. Scabarozzi, S. Amini, P. Finkel, M. W. Barsoum, W. M. Tambussi, J. D. Hettinger, S. E. Lofland, M. Drulis, and H. Drulis, *J. Appl. Phys.* (in press).
- ²⁹S. Gupta, D. Filimonov, and M. W. Barsoum, *J. Am. Ceram. Soc.* **89**, 2974 (2006).
- ³⁰S. Amini, M. W. Barsoum, and T. El-Raghy, *J. Am. Ceram. Soc.* **90**, 3953 (2007).
- ³¹S. Amini, A. Zhou, A. DeVillier, S. Gupta, P. Finkel, and M. W. Barsoum, "Synthesis, Elastic and Mechanical Properties of Cr₂GeC," *J. Mater. Res.* (in press).
- ³²Procedure SETARAM, SETSOFT 2000, V1.2.
- ³³G. Kresse and J. Furthmüller, *Phys. Rev. B* **54**, 11169 (1996).
- ³⁴Materials Design, MEDEA software, Version 2.2.1, Materials Design, Angel Fire, NM.
- ³⁵G. Kresse and D. Joubert, *Phys. Rev. B* **59**, 1758 (1999).
- ³⁶P. E. Blöchl, *Phys. Rev. B* **50**, 17953 (1994).
- ³⁷J. P. Perdew, K. Burke, and M. Ernzerhof, *Phys. Rev. Lett.* **77**, 3865 (1996).
- ³⁸K. Parlinski, Z. Q. Li, Y. Kawazoe, *Phys. Rev. Lett.* **78**, 4063 (1997).
- ³⁹S. Hunklinger and A. K. Raychaudhuri, *Prog. Low Temp. Phys.* **9**, 267 (1986).
- ⁴⁰W. P. Anderson, B. I. Halperin, and C. M. Varma, *Philos. Mag.* **25**, 1 (1972).
- ⁴¹E. R. Gopal, *Specific Heats at Low Temperatures* (Heykood Books, London, 1966).
- ⁴²J. C. Philips, *Phys. Rev. B* **24**, 1744 (1981).
- ⁴³S. R. Kulkarni, M. Merlini, N. Phatak, S. K. Saxena, G. Artioli, S. Amini, and M. W. Barsoum, "On the thermal stability of Ti₂SC in air and inert atmospheres," *J. Alloys Compd.* (in press).